CONF-8611124--4

DE87 007375

CORRELATED DOUBLE ELECTRON CAPTURE IN SLOW, HIGHLY CHARGED ION-ATOM COLLISIONS

N. Stolterfoht
Hahn-Meitner-Institut Berlin, Glienickerstr. 100, D-1000 Berlin 39

C.C. Havener, R.A. Phaneuf, J.K. Swenson, S.M.Shafroth*, and F.W. Meyer

Oak Ridge National Laboratory, Physics Division
P.O. Box, Oak Ridge, TN 37830

Recent measurements [1,2] of autoionization electrons produced in slow, highly charged ion-atom collisions are reviewed. Mechanisms for double electron capture into equivalent and non-equivalent configurations are analyzed by comparing the probabilities for the creation of $L_1L_{23}X$ Coster Kronig electrons and L-Auger electrons. It is shown that the production of the Coster-Kronig electrons is due to electron correlation effects whose analysis leads beyond the independent-particle model. The importance of correlation effects on different capture mechanisms is discussed.

1. Introduction

Currently, there is considerable interest in studying electron correlation effects in atomic systems. These effects are produced by the electron correlation interaction [3] which is due to the difference of the total Hamiltonian of the system and the model (i.e. the Hartree-Fock) Hamiltonian evaluated within the frame work of the independent particle model. In the past, extensive work has been performed studying electron correlation phenomena, e.g. configuration interaction, in separated atoms. More recently attention has been focused on correlations which occur during a collision [4].

There are various methods to observe electron correlation effects in ion-atom collisions. One method is to compare experimental results for an electron in a given system with calculations based on the independent particle model. This method involves certain problems as it relies on both experimental and theoretical values whose accuracies are often not known. In particular, the theoretical results may involve model assumptions other than those of the Hartee-Fock method, since Hartree-Fock calculations for the diatomic collision system are generally tedious.

A more direct method of exploring correlation effects is to study two-electron processes in comparison with the corresponding one-electron processes. In the independent particle approach the probability for a two-electron process is essentially equal to the product of the probabilities for the corresponding one-electron processes. Thus, correlation processes can be verified experimentally by observing deviations from results obtained by means of the factorized probability. In particular, correlation effects can be directly verified when the probability for a two-electron process is observed to be large compared to the product the corresponding one-electron probabilities.

The prominent example for a two-electron process produced by electron correlation, which has predominantly been observed in separated atoms, is the Auger-effect. (The typical Auger width for light atoms is equal to 10^{-2} a.u. which provides an order-of-magnitude estimate for the strength of the electron correlation interaction.) Hence, it is not surprising that correlation processes which occur during the collision are similar to the Auger process. For instance, the resonant transfer-excitation process, studied in detail recently [5,6], is to be regarded as an inverse Auger process. At low collision energies, which are of specific interest here, the transfer excitation process ceases to be 'resonant'; however, it may still be caused by electron correlation effects. [7] Recently, it has been shown by Roncin et al. [8] that the correlated transfer excitation process is important in low-energy Ne^{7+} + He collisions.

The two-electron process which is of primary interest here is double electron capture. In this article a direct method to exhibit correlation effects on double electron capture in slow, highly-charged ion-atom collisions is presented. Primarily, results from Refs. 1 and 2 are reviewed.

II. Correlated Double Electron Capture

Correlated double capture mechanisms have been discussed for high collision energies by Anderson et al. [9] and Datz et al. [10]. For low incident energies Crandall et al. [11] showed that double electron capture in an important process in C^{4+} + He collisions. The experimental data have been found to agree well with theoretical results evaluated by means of electron correlation effects by Kimura and Olson [12] and by Grozdanov and Janev [13]. On the other hand, Niehaus [14] found recently various experimental data for double electron capture in agreement with theoretical results evaluated from an extension of the classical overbarrier model [15] which does not take explicitly electron correlation effects into account. It appears that the results are not yet conclusive in showing the significance of correlation effects in double capture processes

The previous work [11,14] deals with double electron capture processes where the electrons are transferred essentially into the same shell and, hence, configurations of equivalent (or near equivalent) electrons are produced. It is emphasized that the occupation of equivalent electron configurations can arise either from uncorrelated (sequential) electron transfers or from a correlated (simultaneous) two-electron transfer. However, the situation is different for nonequivalent electron configurations in which one electron configuration occupies a lower lying orbital and the second one occupies a Rydberg state. In this case the uncorrelated two-electron transfer is likely to play a minor role since the single-electron transfer process populates selectively only a few (intermediate) states. This selectivity is the outstanding feature of single-electron capture in slow collisions [15]. Hence, the production of the nonequivalent electron configurations is expected to result predominantly from correlated double electron capture [1]. In the following we focus our attention on the analysis of the nonequivalent electron configurations including higher lying Rydberg states.

The principles of our method are illustrated in Fig. 1 which shows the orbital energies for the O^{6+} + He system. In the incident channel two electrons occupy the He 1s orbital whose energy decreases strongly as the internuclear distance decreases. At about 5 a.u. the uncorrelated double capture may occur by mean of two sequential single-electron transitions. As the col-

lision partners continue to approach each other, resonance conditions are created for the correlated double capture process where one electron is transferred to the 2p state and a second electron is tranferred into a Rydberg state.

Winter et al. [16] pointed out another mechanisms which can produce non-equivalent electron configurations. This mechanism shown in Fig. 2 involves a single-electron transfer at about 5 a.u. followed by a correlated transfer-excitation process. At present there is not sufficient experimental and theoretical information available to favour one or the other of the processes shown in Figs. 1 and 2. In any case it is noted that they are rather similar. In particular, the two processes have in common that they are produced by electron-correlation effects.

The correlation processes which occur during the collision may be further examined using the potential curve diagrams given in Fig. 3. The diagrams indicate crossings between states which differ by <u>one</u> spin orbtial (circles) and by <u>two</u> spin orbitals (squares). The have been denoted as diabatic I and diabatic II, respectivly, by Brenot et al. [17]. At the first crossing, transitions are caused by one-electron interaction such as radial coupling whereas a transition of the second type requires a two-electron interaction such as electron correlation (assuming orthogonal states).

It is important to note that the occurrence of the resonant condition in Fig. 1 corresponds to a crossing in the corresponding potential curve diagram (Fig. 3a). The system $(O + He)^{6+}$ involves an infinite number of such crossings between the entrance channel $O^{6+} + He(1s^2)$ and exothermic exit channels leading to the nonequivalent electron configuration $1s^2 2pn\ell$ in O^{4+}. It is noted that the latter channels with $n > 6$ are located in the cross-hatched area shown in Fig. 3a.

The double capture process indicated in Fig. 2 corresponds to the single-electron transitions into the state represented by the dashed curve attributed asymtotically to $O^{5+}(3d) + He^{+}(1s)$ (Fig. 3). It is followed by the correlated transfer-excitation transition into the states represented by the $1s^2 2pn\ell$ curves in the cross-hatched area. It is seen from Fig. 3a that all these transitions takes place in a rather narrow region of internuclear distances near 4 to 5 a.u.

To show that correlation effects are important for the population of certain configurations during the collision, one has to make sure that correlation effects do not produce these configurations after the collision. There, a nonequivalent electron configuration could in principle be populated by electron correlation interaction with the corresponding equivalent electron configuration. It is recalled that the strength of the electron correlation interaction [3] is of the order of 10^{-2} a.u. Hence, to create considerable configuration mixing it is required that the energy seperation of the configurations involved is close to this value. However, in O^{4+} the energy differences between the $1s^2 2p n\ell$ and $1s^2 3\ell 3\ell'$ configurations are about 0.5 a.u. (Fig. 3a) so that the configuration interaction is expected to be small in this case.

On the other hand, coupling to the continuum configurations is important since they are degenerate with the bound state configurations considered here. Thus, after the collisions the doubly excited projectiles decay by autoionization, ejecting an electron. From Figs. 1 and 2 it is seen that the equivalent electron configurations $1s^2 3\ell n\ell'$ gives rise to L-Auger electrons whereas the nonequivalent electron configurations $1s^2 2p n\ell$ result in Coster-Kronig electrons. Hence, the different double capture processes can be analyzed by means of high resolution electron spectroscopy. Auger electron measurements for slow, highly ionized collision systems have first been performed by Bordenave-Montesquieu et al. [19]. Similar experiments have recently been made by Gleizes et al. [20], Mack et al. [21], Stolterfoht et al. [1], Meyer at al. [2], and Mann [22].

III. Experimental Results and Discussion

In our work [1,2] we measured electron spectra with high resolution using the method of zero-degree Auger spectroscopy [6,18]. This method has the advantage that kinematic broadening effects are unimportant. Fig. 4 shows the electron spectra for the O^{6+} + He system covering Coster-Kronig and L-Auger electrons. The L-Auger electrons are due to the configurations $1s^2 3\ell n\ell'$ which are likely to be produced by uncorrelated electron transfers. However, as pointed out above, these equivalent electron configurations may also be created by correlated two-electron transitions [12,13]. In particular, close

inspection of Fig. 3a indicates that in the population of $1s^2 3\ell n\ell'$ with $n > 4$ correlation effects are expected to play a significant role. Further work is suggested to study correlation effects on the formation of the near equivalent electron configurations.

It is recalled that the Coster Kronig electrons provide a direct measure for the significance of the correlation effects. In Fig. 5 the Coster-Kronig lines are shown in greater detail. For the O^{4+} ion it is noted that autoionization of the $1s^2 2pn\ell$ states becomes energetically allowed for $n > 6$. The oxygen impact data show that the population of the nonequivalent configurations $1s^2 2pn\ell$ are significant for the whole Rydberg series (Fig. 5).

On the contrary for C^{4+} impact the Coster-Kronig lines are seen to be weak. This can be understood in terms of the potential diagram in Fig. 3c. From the cross hatched area it is seen that the $1s^2 2pn\ell$ channels are endothermic and, thus, do not lead to crossings with the incident channel $C^{4+} + He(1s^2)$. However, intense Coster-Kronig lines are expected and observed for the $C^{4+} + H_2$ system where, because of the reduced target ionization potential, crossings leading to the configurations $1s^2 2pn\ell$ are present. The experimental results for the Coster-Kronig and L-Auger electrons are shown in Fig. 6. It is seen that the Coster-Kronig electrons from the system $C^{4+} + H_2$ contribute a significant fraction to the total intensity.

From the observed electron yields, absolute cross sections for electron emission were evaluated. Referring back to the system $O^{6+} + He$ (Fig. 4) the values $1.3\ 10^{-16}$ cm^2 and $2.2\ 10^{-16}$ cm^2 were determined for the production of $L_1L_{23}X$ Coster Kronig electrons and L-Auger electrons, respectively [23]. These results refer to the projectile frame of reference where the electrons emission is assumed to be isotropic. Hence we obtain the cross section fraction of 40 % for the Coster Kronig electrons. This significant fraction has led us to the conclusion that correlations effects are important for double electron capture in slow, highly charged ion-atom collisions [1].

The fraction of 40 % has been confirmed for the system 120-keV $O^{6+} + He$ measured by Mann [22] at 0° observation angle as in our work [1,2]. However, Mack and Niehaus [24] and Bordenave-Montesquieu et al. [25] have measured the electrons at 50° and 150°, respectively, and have obtained a cross section

fraction for the Coster Kronig electrons of about 10 %. We would not expect that experimental effects are fully responsible for the observed discrepancies.

Hence, the possibility of anisostropies in the emission of the electrons must be considered. For the L-Auger electrons Bordenave-Montesquieu et al. [26] found within an angular range of 10° to 160° rather weak anisotropies in the electron emission from low-energy collisions of N^{6+} and N^{7+} on He. However, the angular distribution of the Coster Kronig electrons may be quite different. The Coster Kronig transitions under study here involve exclusively final S states such that the full angular momentum of the intermediate state is carried to the continuum. Also with respect to the observed discrepancies in the relative intensities of the Coster Kronig electrons it would be useful to include the observation angle of 0° in the angular distribution measurements.

From the experimental data available at present it is concluded that for the cross section fraction for the Coster Kronig electrons lies probably between 10 % and 40 % corresponding to absolute cross sections of $0.3 \cdot 10^{-16}$ cm^2 to $1.3 \cdot 10^{-16}$ cm^2. These values refer to the whole $1s^2 2pn\ell$ Rydberg series with $n > 6$. The cross sections have to be devided by a factor of 5 when only the first (observable) member of the series is considered, i.e. $1s^2 2p6\ell$.

To see if the experimental values can be predicted theoretically, an order-of-magnitude estimate of the cross section σ for correlated double capture was performed by means of the Landau-Zener formula [27]. For small transition probabilities one obtains the approximate relation:

$$\sigma \approx R_c^2 \, 2\pi^2 \, \frac{H_{12}^2}{v \, F}$$

where R_c is the crossing radius, H_{12} is the coupling matrix element, v is the collision velocity and F is the derivative of the energy difference of the diabatic potential curves involved (Fig. 3). With the reasonable choice of $H_{12} = 10^{-2}$ a.u. one obtains $6 \cdot 10^{-18}$ cm^2 for the population of the

$1s^2 2p6\ell$ configuration. This value lies near the lower limit of the experimental results noted above.

Results similar to those for O^{6+} + He are found for the systems N^{5+} + He, N^{5+} + H_2, and C^{4+} + H_2 for which significant Coster Kronig lines have been observed [1,2,24,25]. This shows that correlation effects contribute considerably to the double capture process in various low-energy collision systems. It is difficult, however, to generalize the role of correlation effects for other collision systems. Roncin et al. [28] found only weak correlation effects for the impact of various ions with charge state $q > 7$. This finding is consistent with our study [2] of O^{7+} + He which shows a factor of about 2 smaller cross section fraction for the Coster Kronig electrons than for O^{6+} + He.

In conclusion, it is found that the charge state of the projectile as well as the ionization potential of target atom has significant influence on the production of the Coster Kronig electrons. It appears that the role of correlation effects in double capture processes depends critically on the collision system. Future work is needed to allow conclusions about the systematics of the correlation effects in slow, highly charged ion-atom collisions. In particular, theoretical work is needed to fully verify the proposed correlation processes.

Acknowledgement

We are indebted to Dr. Arendt Niehaus for clarifying discussions and to Drs. John Tanis and Bill Graham for valuable comments on the manuscript. We thank Drs. H. Winter, M. Mack, A. Bordenave-Montesquieu, and R. Mann for informing us about their data prior to publication. This work was sponsered by the Divsion of Chemical Science, U.S. Department of Energy, under Contract No. DE-AC05-84OR21400 with Martin Marietta Energy Systems, Inc.

* Permanent Adress: University of North Carolina, Chapel Hill, N.C. 27514 and Triangle Universities Nuclear Physics Laboratory, Durham, N.C. 27706

References

[1] N. Stolterfoht, C.C. Havener, R.A. Phaneuf, J.K. Swenson, S.M. Shafroth, and F.W. Meyer, Phys. Rev. Lett. 57 (1986) 74

[2] F.W. Meyer C.C. Havener, R.A. Phaneuf, J.K. Swenson, S.M. Shafroth, and N. Stolterfoht, Ninth Conference of Application of Accelerators in Research and Industry, Invited Paper, to be published in Nuclear Instruments and Methods

[3] The electron correlation interaction is part of the electron-electron interaction whose partition into different terms may be performed using the projection operator method given by H. Feshbach, Ann. Phys. (N.Y.) 5 (1958) 537

[4] J.F. Reading, A.L. Ford, J.S. Smith, R.L. Becker, Electronic and Atomic Collisions, Invited Papers, edited by J. Eichler, I.V. Hertel and N. Stolterfoht (North Holland, Amsterdam, 1984) p. 201

[5] J.A. Tanis, E.M. Bernstein, W.G. Graham, M.P. Stöckli, M. Clark, R,.H, McFarland, T.J. Morgan, K.H. Berkner, A.S. Schlachter, and J.W. Stearns, Phys. Rev. Lett. 53 (1984) 2551

[6] A. Itoh, T.J. Zouros, D. Schneider, U Stettner, W. Zeitz and N. Stolterfoht, J. Phys. B 18 (1985) 4581

[7] M. Kimura, T. Iwai, Y. Kaneko, N. Kobayashi, A. Matsumoto, S. Ohtani, K. Okuno, S. Takagi, H. Tawara, and S. Tsurubuchi, J. Phys. B 15 (1982) L851

[8] P. Roncin, M.N. Gariboriaud, H. Laurent, and M. Barat, J. Phys. B 19 (1986) L691

[9] L.H. Andersen, M. Frost, P. Hvelplund, H. Knudsen, and S. Datz, Phys. Rev. Lett. 52 (1984) 518

[10] S. Datz, C. Bottcher, L.H. Andersen, P. Hvelplund, and H. Knudsen, Nucl. Instrum. Methods Phys. Res. B10/11 (1985) 116

[11] D.H. Crandall, R.E. Olson, E.J. Shipsey, and J.C. Browne, Phys. Rev. Lett. 36 (1976) 858

[12] M. Kimura and R.E. Olson, J. .hys. B 18 (1984) L713

[13] T.P. Grozdanov and R.K. Janev, J. Phys. B 13 (1980) 3431

[14] A. Niehaus, J. Phys. B 19 (1986) 2925

[15] H. Ruyfuku, K. Sasaki, and T. Watanabe, Phys. Rev. A 21 (1980) 745

[16] H. Winter, M. Mack, R. Hoekstra, A. Niehaus, and F.J. de Heer, (1986), private communicaton

[17] J.C. Brenot, D. Dhuicq, J. P. Gauyacq, J. Pommier, V. Sidis, M. Barat, and E. Pollack, Phys. Rev. A 11 (1975) 1933

[18] N. Stolterfoht, A. Itoh, D. Schneider, Th. Schneider, G. Schiwietz, H. Platten, G. Nolte, R. Glodde, U. Stettner, W. Zeitz, and T.J.M Zouros, International Conference on X-Ray and Inner-Shell Processes in Atoms, Molcules, and Solids, Invited Lecture, edited by A. Meisel (University Press, Leipzig, 1984) p. 1983

[19] A. Bordenave-Montesquieu, P. Benoit-Cattin, A. Gleize, A.I. Marakchi, S. Dousson, and D. Hitz, J. Phys. B 17 (1984) L127 and L223

[20] A. Gleizes, P. Benoit-Cattin, A. Bordenave-Montesquieu, S. Dousson, and D. Hitz, Electronic and Atomic Collisions, Abstract of Contributed Papers, Edited by M.J. Coggiola, D.L. Huestis, R.P. Saxon (Palo Alto, 1985) p. 464

[22] R. Mann, J. Phys. Rev. A., to be published

[23] It is noted that our cross sections given in Ref. 1 must be increased by a factor of 4 due to a normalization error. Corrected cross sections are given in Ref. 2.

[24] M. Mack and A. Niehaus (1986) private communication

[25] A. Bordenave-Montesquieu et al. (1986) private communication

[26] A. Bordenave-Montesquieu, P. Benoit-Cattin, A. Gleizes, S. Dousson, and D. Hitz, Electronic and Atomic Collisions, Abstracts of Contributed Papers, edited by M.J. Coggiola, D.L. Huestis, and R.P. Saxon, (Palo Alto, 1985) p. 465

[27] C.D. Landau, J. Phys. (USSR) 2 (1932) 46 and C. Zener, Proc. Roy. Soc. A 137 (1932) 696

[28] P. Roncin, M. Barat, and H. Laurent, Europhys. Lett. 2 (1986) 371

Figure Caption

Fig. 1 Diagram of orbital energies for the systems O^{6+} + He. The electron binding energies in O^{5+} are obtained from the Rydberg formula $B_n = Q^2/2n^{*2}$ where Q is the charge of the atomic core seen by the Rydberg electron and the principal quantum number n^* involves an appropriate quantum defect. The diagram shows the uncorrelated two-electron capture in the n = 3 shell at about 5 a.u. and the correlated two-electron capture populating the $1s^2 2pn\ell$ configuration. From Ref. 1

Fig. 2 Diagram of orbital energies for the system O^{6+} + He as in Fig. 1. The diagram indicates, apart from the uncorrelated two-electron capture into the n = 3 shell, a single-electron capture followed by a correlated transfer-excitation process populating the $1s^2 2pn\ell$ configuration.

Fig. 3 Potential curve diagrams for the systems O^{6+} + He, N^{5+} + He, and C^{4+} + He. The diagram is based on calculations performed similarly as for Fig. 1.

Fig. 4 Spectrum of $L_1L_{23}X$ Coster Kronig electron and L-Auger electrons for the 60-keV O^{6+} + He collisions. The relative cross sections and the energy scale refer to the projectile frame of reference. The Coster Kronig electrons and L Auger electrons are obtained with and without preacceleration (see Ref. 1), respectively.

Fig. 5 Spectra of $L_1L_{23}X$ Coster Kronig electrons produced in 60-keV O^{6+} + He and 40-keV C^{4+} + He collisions. The relative cross sections and the energy scale refer to the projectile frame of the reference. From Ref. .

Fig. 6 Spectrum of $L_1L_{23}X$-Coster Kronig electron and L-Auger electrons for the 40-keV C^{4+}+ He collisions. The relative cross sections and the energy scale to the projectile frame of reference. The whole spectrum is obtained in one run using the preacceleration method described in Ref. 1.

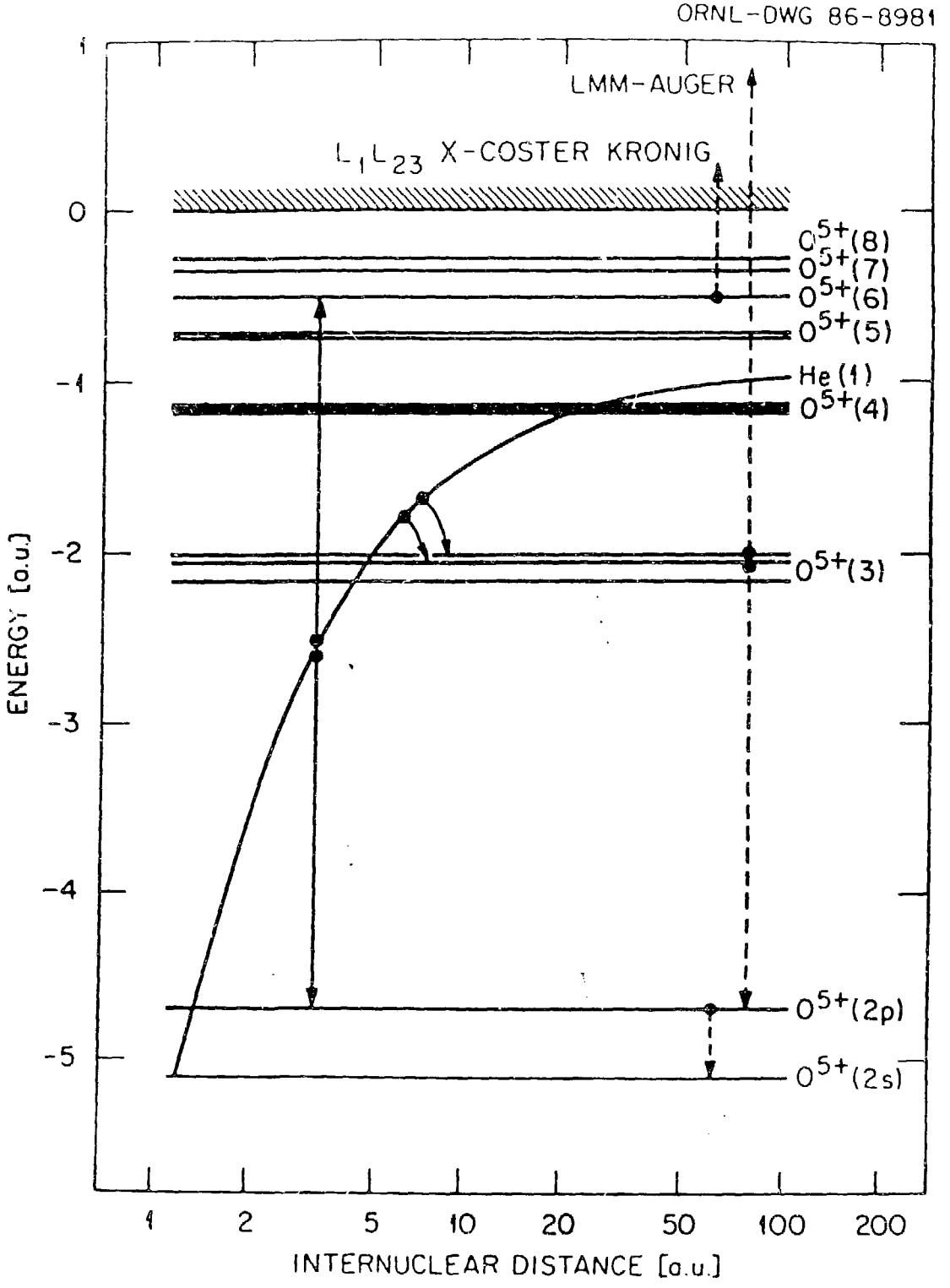
ORNL-DWG 86-8981
LMM-AUGER
L_1L_{23} X-COSTER KRONIG
$O^{5+}(8)$
$O^{5+}(7)$
$O^{5+}(6)$
$O^{5+}(5)$
He(1)
$O^{5+}(4)$
$O^{5+}(3)$
$O^{5+}(2p)$
$O^{5+}(2s)$
ENERGY [a.u.]
0
-1
-2
-3
-4
-5
1
2
5
10
20
50
100
200
INTERNUCLEAR DISTANCE [a.u.]

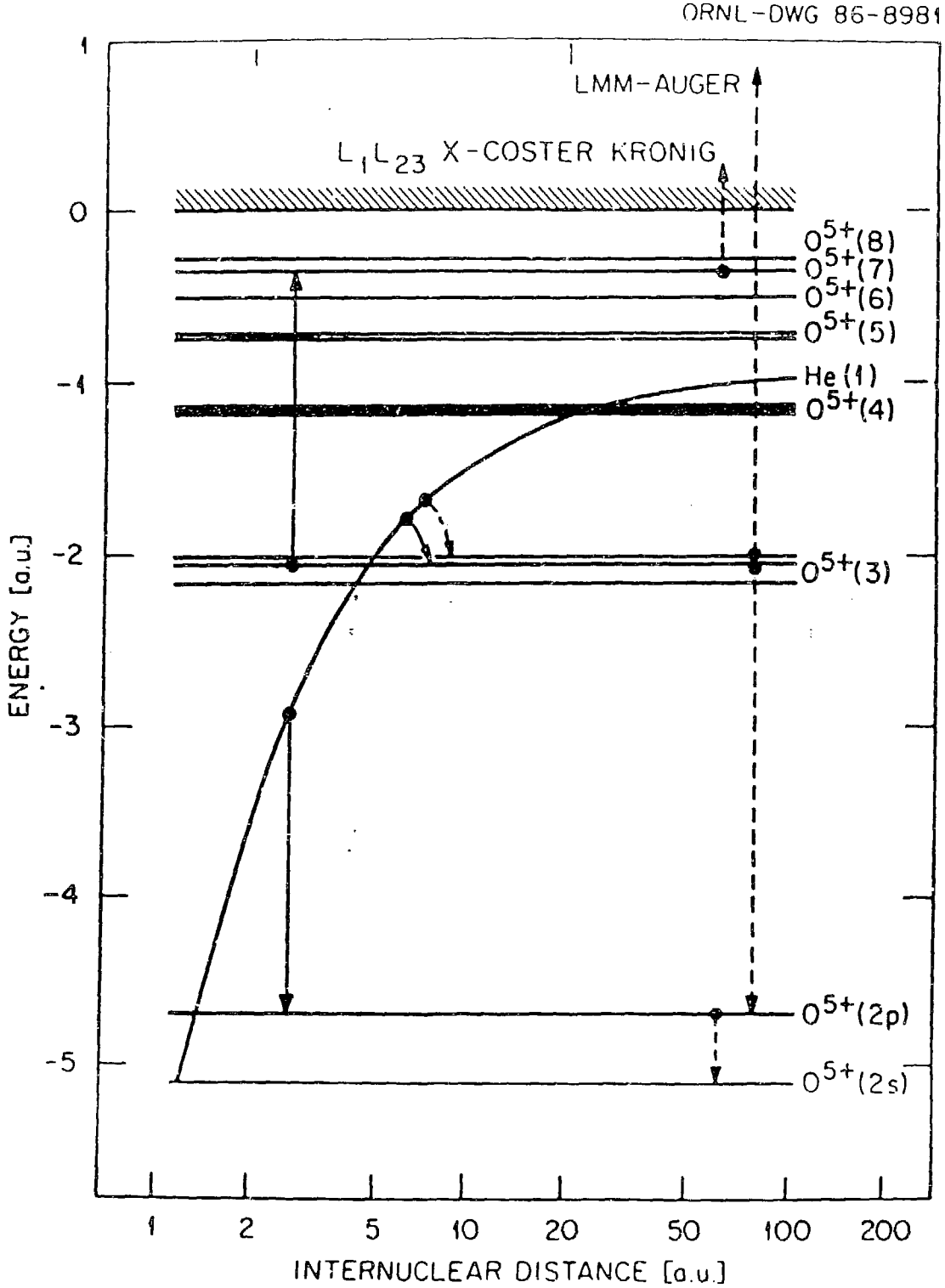
ORNL-DWG 86-8981
LMM-AUGER
L_1L_{23} X-COSTER KRONIG
$O^{5+}(8)$
$O^{5+}(7)$
$O^{5+}(6)$
$O^{5+}(5)$
He(1)
$O^{5+}(4)$
$O^{5+}(3)$
$O^{5+}(2p)$
$O^{5+}(2s)$
ENERGY [a.u.]
1
0
-1
-2
-3
-4
-5
1
2
5
10
20
50
100
200
INTERNUCLEAR DISTANCE [a.u.]

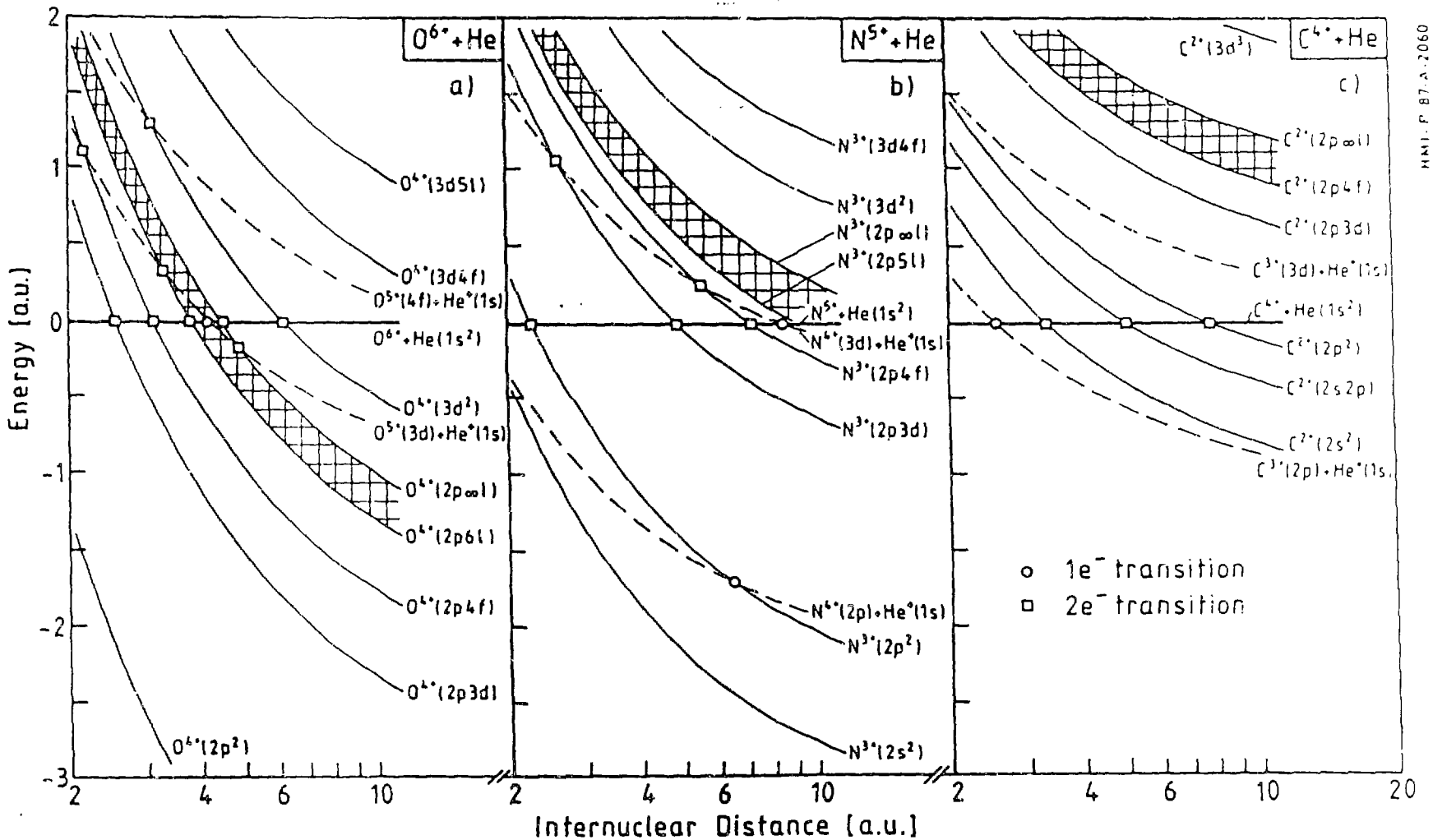
O^{6+}+He
a)
O^{5+}(3d5l)
O^{5+}(3d4f)
O^{5+}(4f)+He^{+}(1s)
O^{6+}+He($1s^2$)
O^{4+}($3d^2$)
O^{5+}(3d)+He^{+}(1s)
O^{4+}(2p∞l)
O^{4+}(2p6l)
O^{4+}(2p4f)
O^{4+}(2p3d)
O^{4+}($2p^2$)
N^{5+}+He
b)
N^{3+}(3d4f)
N^{3+}($3d^2$)
N^{3+}(2p∞l)
N^{3+}(2p5l)
N^{5+}+He($1s^2$)
N^{4+}(3d)+He^{+}(1s)
N^{3+}(2p4f)
N^{3+}(2p3d)
N^{4+}(2p)+He^{+}(1s)
N^{3+}($2p^2$)
N^{3+}($2s^2$)
C^{4+}+He
c)
C^{2+}($3d^3$)
C^{2+}(2p∞l)
C^{2+}(2p4f)
C^{2+}(2p3d)
C^{3+}(3d)+He^{+}(1s)
C^{4+}+He($1s^2$)
C^{2+}($2p^2$)
C^{2+}(2s2p)
C^{2+}($2s^2$)
C^{3+}(2p)+He^{+}(1s)
1e⁻ transition
2e⁻ transition
Energy [a.u.]
Internuclear Distance [a.u.]
HMI-P 87-A-2060

Fig.3

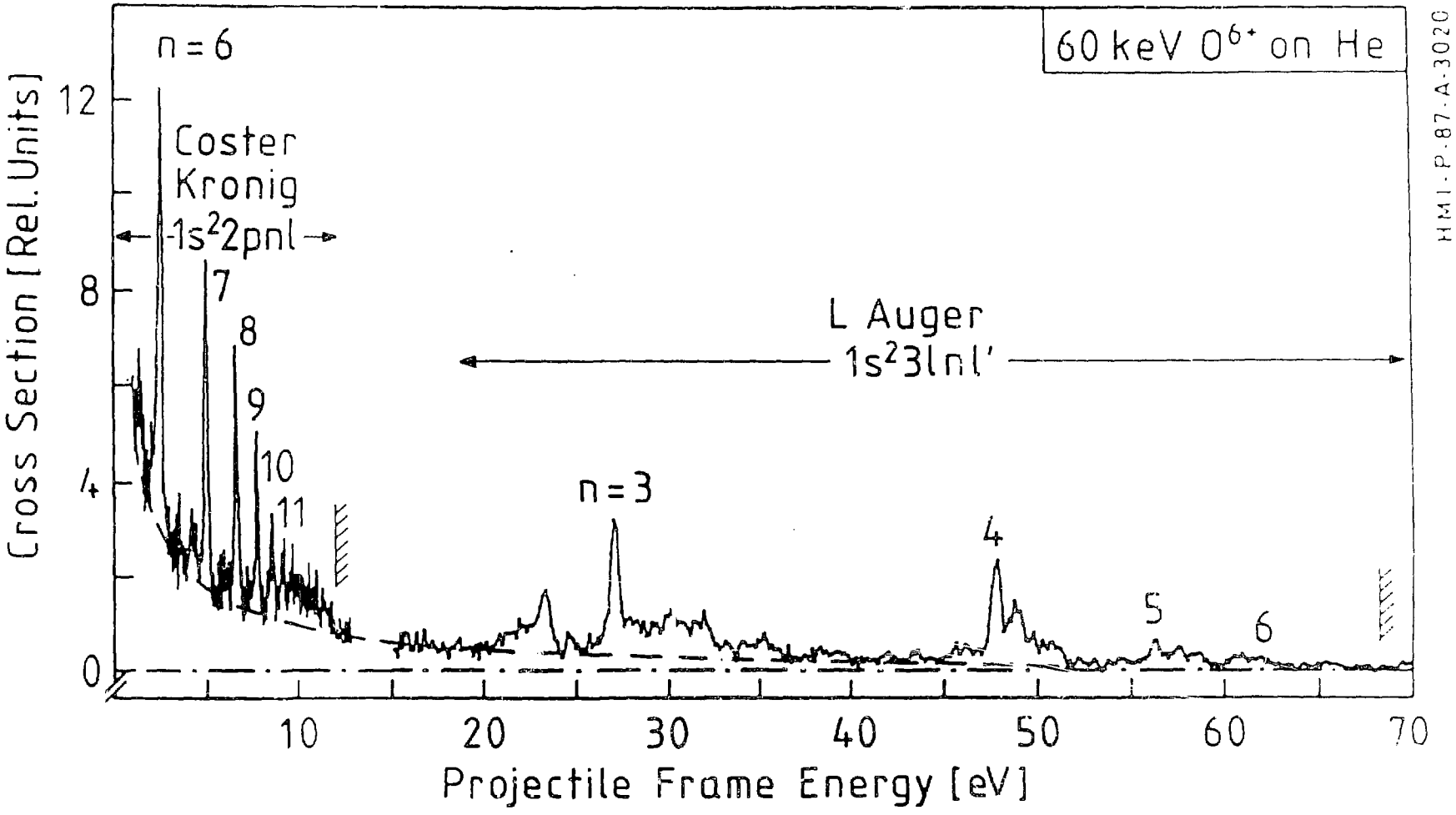
n = 6
60 keV O^{6+} on He
Coster
Kronig
$1s^2 2pnl$
7
8
9
10
11
L Auger
$1s^2 3lnl'$
n = 3
4
5
6
Cross Section [Rel. Units]
12
8
4
0
10
20
30
40
50
60
70
Projectile Frame Energy [eV]
HMI-P-87-A-3020

Fig. 4

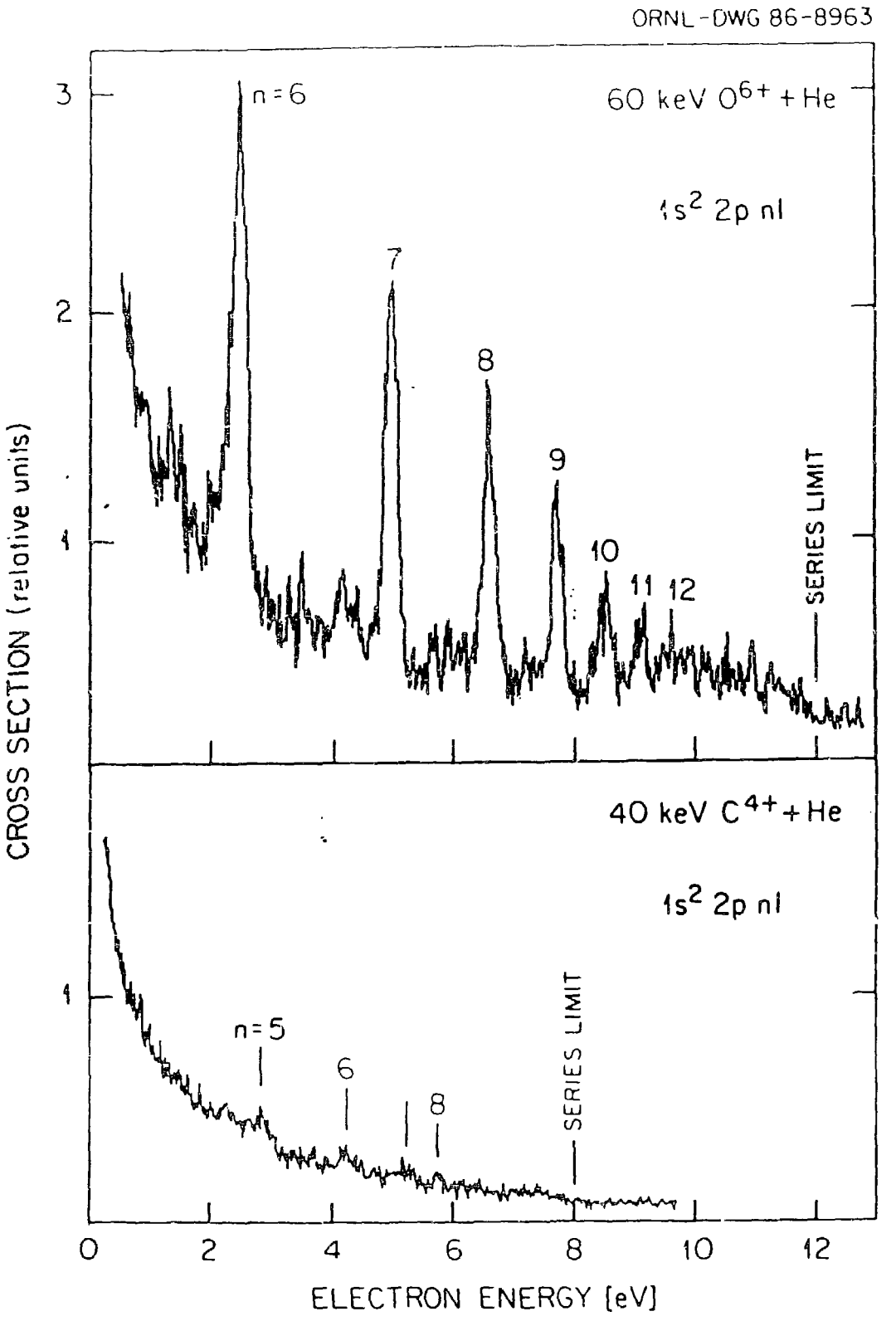
ORNL-DWG 86-8963
60 keV O^{6+} + He
$1s^2$ 2p nl
n=6
7
8
9
10
11
12
SERIES LIMIT
40 keV C^{4+} + He
$1s^2$ 2p nl
n=5
6
8
SERIES LIMIT
CROSS SECTION (relative units)
3
2
1
1
0
2
4
6
8
10
12
ELECTRON ENERGY [eV]

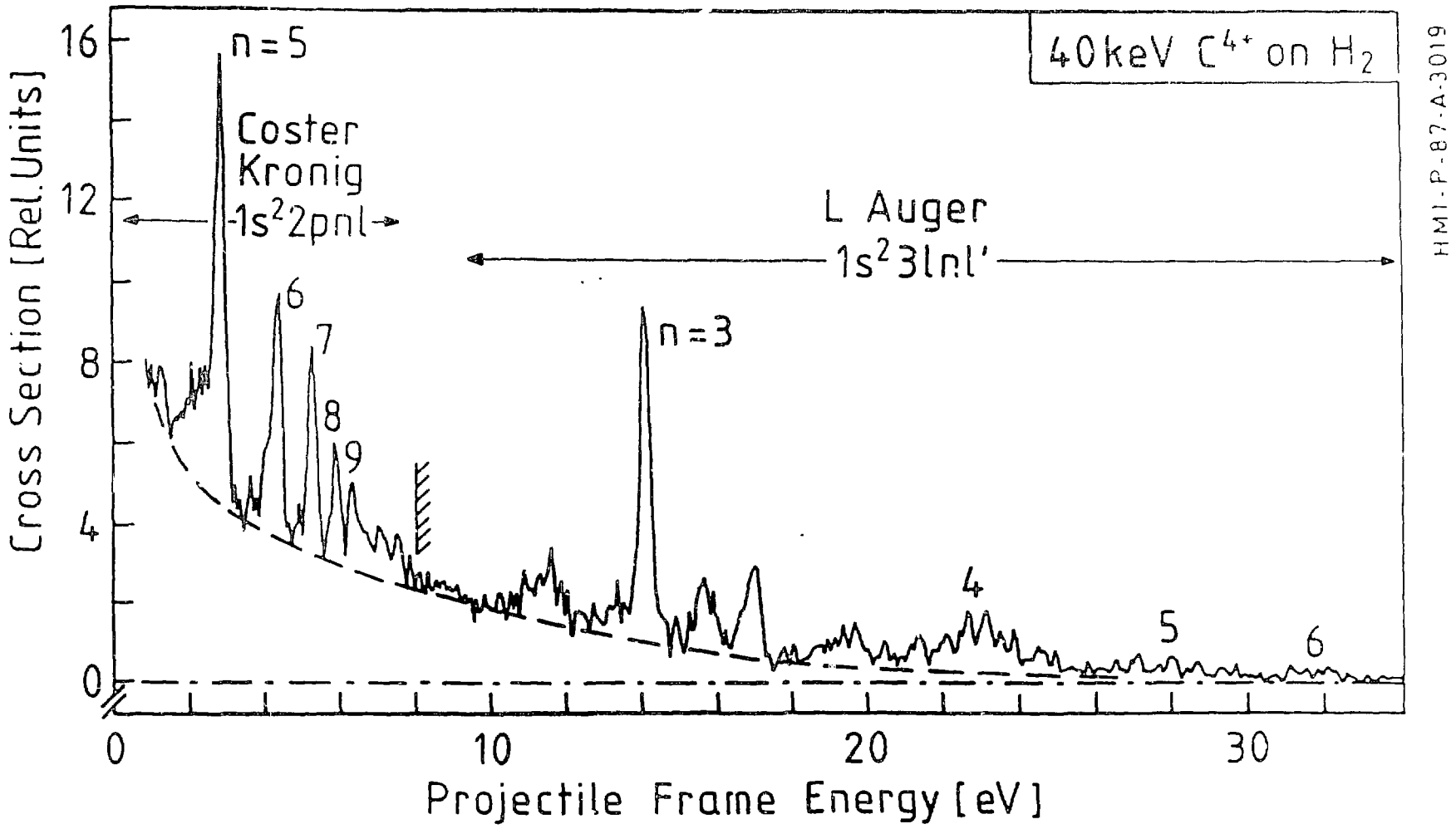
40keV C4+ on H2
n=5
Coster
Kronig
-1s²2pnl-
L Auger
1s²3lnl'
n=3
6
7
8
9
4
5
6
16
12
8
4
0
0
10
20
30
Cross Section [Rel.Units]
Projectile Frame Energy [eV]
HMI-P-87-A-3019

Fig. 6

DISCLAIMER